Estimation of Relative Source Locations From Seismic Amplitude: Application to Earthquakes and Tremors at Meakandake Volcano, Eastern Hokkaido, Japan

Masashi Ogiso (mogiso@mri-jma.go.jp)
Meteorological Research Institute, Japan Meteorological Agency, 1-1 Nagamine, Tsukuba, 305-0052, Japan https://orcid.org/0000-0003-4970-3834

Kiyoshi Yomogida
Hokkaido University Faculty of Science

Express Letter

Keywords: Relative source location, Seismic amplitude, Volcano-tectonic earthquakes, Volcanic tremors, Tremor 25 migration, Meakandake volcano

Posted Date: October 23rd, 2020

DOI: https://doi.org/10.21203/rs.3.rs-95632/v1

Version of Record: A version of this preprint was published on January 29th, 2021. See the published version at https://doi.org/10.1186/s40623-021-01366-8.

Estimation of relative source locations from seismic amplitude: application to earthquakes and tremors at Meakandake volcano, eastern Hokkaido, Japan

Masashi Ogiso, Meteorological Research Institute, Japan Meteorological Agency, 1-1 Nagamine, Tsukuba, 305-0052, Japan, mogiso@mri-jma.go.jp

Kiyoshi Yomogida, Department of Earth and Planetary Science, Faculty of Science, Hokkaido University, North 10 West 8, Kita-ku, Sapporo, 060-0810, Japan, yomo@sci.hokudai.ac.jp

Corresponding author: Masashi Ogiso

Preprint submitted to *Earth, Planets and Space* on October 16, 2020

Abstract

Although seismic amplitudes can be used to estimate event locations for volcanic tremors and other seismic events with unclear phase arrival times, the precision of such estimates is strongly affected by site amplification factors. Therefore, reduction of the influence of site amplification will allow more precise estimation of event locations by this method. Here, we propose a new method to estimate relative event locations using seismic amplitudes. We use the amplitude ratio between two seismic events at a given station to cancel out the effect of the site amplification factor at that station. By assuming that the difference between the hypocentral distances of these events is much smaller than their hypocentral distances themselves, we derive a system of linear equations for the differences in relative event locations. This formulation is similar to that of a master event location method that uses differences in phase arrival times. We applied our new method to earthquakes and tremors at Meakandake volcano, eastern Hokkaido, Japan. Comparison of the hypocentral distributions of volcano-tectonic earthquakes obtained thereby with those obtained from phase arrival times confirmed the validity of our new method. Moreover, our method clearly identified source migration among three source regions in the tremor on 16 November 2008, consistent with previous interpretations of other geophysical observations in our study area. Our method will thus be useful for detailed analyses of seismic events whose onset times are ambiguous.

Keywords

Relative source location, Seismic amplitude, Volcano-tectonic earthquakes, Volcanic tremors, Tremor migration, Meakandake volcano

Introduction

Estimating the location of seismic events is a fundamental step in seismological analyses. Phase arrival times are routinely used to locate earthquake hypocenters (e.g., Hirata and Matsu'ura 1987; Klein 2002). Several other techniques have been applied, some of which have dealt successfully with ambiguous arrival times. Seismic array observations (e.g., Rost and Thomas 2002) enable us to estimate wave propagation direction and apparent velocity by using waveform similarity (e.g., Capon 1969; Neidell and Taner 1971; Goldstein and Archuleta 1987), which can be used to estimate a waveform's point of origin. When waveforms are not similar among stations, but seismogram envelopes are, differences in phase arrival times among stations can be estimated from seismogram envelope correlations, and source locations can be estimated from these arrival-time differences; this is known as the envelope correlation method (Obara 2002).

Seismic amplitude can also be used to estimate seismic event locations. The amplitude source location (ASL) method (e.g., Battaglia and Aki 2003; Battaglia et al. 2005; Kumagai et al. 2010) uses amplitude spatial decay for this purpose. Because the ASL method does not rely on phase arrival times, it is applicable to seismic events with unclear onset times, such as tremors. The ASL method has been applied to tremors and earthquakes within volcanoes (Battaglia 2003; Kumagai et al. 2011; Ogiso and Yomogida 2012; Kumagai et al. 2013a; Ogiso et al. 2015; Kurokawa et al. 2016; Ichihara and Matsumoto 2017; Walsh et al. 2017; Ichimura et al. 2018; Kumagai et al. 2019), pyroclastic flows (Yamasato 1997; Jolly et al. 2002), lahars or debris flows (Kumagai et al. 2009; Ogiso and Yomogida 2015; Doi and Maeda 2020), and snow avalanches (Pérez-Guillén et al. 2019). The ASL method has also revealed the source process of a large subduction zone earthquake (Kumagai et al. 2013b), the detailed distribution of shallow low-frequency earthquakes near a trench axis (Tamaribuchi et al. 2019). Because the ASL method uses observed seismic amplitudes, the appropriate correction of site amplification effects is important for the accuracy of event locations determined by this method (Kumagai et al. 2013a).

In addition to estimating absolute source locations, as discussed above, estimates of relative source location have been used to derive precise location distributions. The underlying concept for this techniques is the removal of common factors that affect location precisions. A joint hypocenter determination technique (e.g., Douglas 1967) includes site correction terms in a system of equations designed to simultaneously estimate relative event locations and site correction terms. A master event location method (Aoki 1974; Ito 1985; Frémont and Malone 1987) attributes differences between phase arrival

times of a reference event and other events to differences in their relative locations. When seismic events occur in close proximity to one another, the errors arising from wave propagation path can be canceled out by accounting for arrival-time differences. A double-difference earthquake location algorithm (Waldhauser and Ellsworth 2000) is a novel approach to source-location estimation that uses the differences of observed and theoretical arrival times between event pairs to minimize the influence of an unmodeled heterogeneous velocity structure without any reference events. These techniques for estimating relative source locations have revealed more detailed spatial characteristics of seismicities than those by absolute location estimation methods.

Here, we propose a new method to estimate relative source locations that uses seismic amplitudes and takes advantage of aspects of both the ASL method and the relative location methods. Our method uses amplitude ratios between reference and other events at several stations to cancel out the effects of site amplification. By assuming that subevents occur near a reference event, we derive a system of linear equations for differences in relative location. We then estimate relative locations by solving the equations with a standard least-squares method. In this paper, we first explain the formulation of our new method and then apply it to volcano-tectonic (VT) earthquakes and tremors at Meakandake volcano, eastern Hokkaido, Japan. To test the validity of our method, we then compare the hypocentral distribution of VT earthquakes derived by our new method with those derived by two methods that determine hypocenters from phase arrival times. Next, we demonstrate that the migration of the tremor locations that we identified with our new method is clearer than that in the previous study (Ogiso and Yomogida 2012), and discuss the relationship between tremor source regions and other geophysical observations.

Theoretical background

In this section, we briefly review the ASL method and then present the theory that underpins our new method of determining relative source locations from seismic amplitudes.

ASL method

When body waves propagate, the observed seismic amplitude $A_i(f)$ at a certain frequency f at the ith station can be represented as

$$A_i(f) = A_0(f)\frac{\exp(-B(f)r_i)}{r_i}S_i(f), \tag{1}$$

where $A_0(f)$ is the source radiation amplitude, r_i the hypocentral distance between the source and the ith station, and $S_i(f)$ the site amplification factor at the ith station. $B(f)$ is defined as

$$B(f) = \frac{\pi f}{Q\beta}, \tag{2}$$

where Q is the intrinsic attenuation factor and β the velocity of the medium, or the average S-wave velocity in general. If we assume the source location for a certain event, we can calculate the source radiation amplitude $A_0(f)$ as

$$A_0(f) = \frac{1}{N}\sum_{i=1}^{N}\frac{A_i(f)}{S_i(f)} r_i \exp(B(f)r_i), \tag{3}$$

where N is the number of observations. Using equations (1) and (3), we calculate the normalized residual R as

$$R = \frac{\sum_{i=1}^{N}\{A_i(f)/S_i(f) - A_0(f)\exp(-B(f)r_i)/r_i\}^2}{\sum_{i=1}^{N}\{A_i(f)/S_i(f)\}^2}. \tag{4}$$

In application of the ASL method, a grid search is usually conducted to find the location where R reaches its minimum value. Because the heterogeneous radiation pattern of the source is not modeled in equation (1), and because distortion of the radiation pattern becomes more obvious in higher frequency ranges (e.g., Takemura et al. 2009; Kobayashi et al. 2015), seismic amplitudes at high frequencies (usually higher than 5 Hz) are suitable for the ASL method.

Estimation of relative source locations from seismic amplitudes

As shown by equation (3), the site amplification factor $S_i(f)$ has a large influence on source locations estimated by the ASL method. The coda normalization method (e.g., Phillips and Aki 1986; Takemoto et al. 2012) is widely used to estimate site amplification factors. Calibration of site amplification factors with seismic events for which locations are well-constrained (Ichihara and Matsumoto 2017; Walsh et al. 2017; Kumagai et al. 2019) is preferable when estimating source locations. Nevertheless, some uncertainties are unavoidable when estimating site amplification factors. In this study, we propose the use of amplitude ratios to cancel out uncertainties in site amplification factors.

From equation (1), the amplitude ratio between two events, the jth and kth events, at the ith station is

$$\frac{A_i^j(f)}{A_i^k(f)} = \frac{A_0^j(f)}{A_0^k(f)}\frac{\exp(-B(f)r_{ij})}{\exp(-B(f)r_{ik})}\frac{r_{ik}}{r_{ij}}, \tag{5}$$

where $A_i^j(f)$ and $A_i^k(f)$ are the observed amplitudes of the jth and kth events at the ith station, $A_0^j(f)$ and $A_0^k(f)$ are the source radiation amplitudes of the jth and kth events, respectively, and r_{ij} and r_{ik}

are the hypocentral distances from the ith station to the jth and kth events, respectively. We define the difference of the hypocentral distances of the jth and kth events Δr_{jk} as

$$\Delta r_{jk} = r_{ik} - r_{ij}, \tag{6}$$

and, substituting equation (6) into (5) gives

$$\frac{A_i^j(f)}{A_i^k(f)} = \frac{A_0^j(f)}{A_0^k(f)} \frac{1}{\exp(-B(f)\Delta r_{jk})} \left(1 + \frac{\Delta r_{jk}}{r_{ij}}\right). \tag{7}$$

Here we assume that the sources of the jth and kth events are near each other so that Δr_{jk} becomes much smaller than the hypocentral distances r_{ij} and r_{ik}. Taking the natural logarithm of both sides of equation (7) and approximating $\ln(1 + \Delta r_{jk}/r_{ij})$ as $\Delta r_{jk}/r_{ij}$, equation (7) becomes

$$\ln \frac{A_i^j(f)}{A_i^k(f)} \approx \ln \frac{A_0^j(f)}{A_0^k(f)} + B(f)\Delta r_{jk} + \frac{\Delta r_{jk}}{r_{ij}}. \tag{8}$$

Similar to the formulation of Aoki (1974) for a master event location method using differences of phase arrival times, we can approximate Δr_{jk} to be

$$\Delta r_{jk} \approx \mathbf{n}_i^j \cdot \Delta \mathbf{x}_k, \tag{9}$$

where $\mathbf{n}_i^j$ is the unit vector representing the takeoff angle and azimuth from the jth event to the ith station, and $\Delta \mathbf{x}_k$ is the location vector of the kth event relative to the jth event. After substituting equation (9) into (8), we rewrite equation (8) into the following matrix form for standard least-square inversion:

$$\mathbf{d} = \mathbf{G}\mathbf{m}, \tag{10}$$

where $\mathbf{d}$ represents the data vector consisting of $\ln(A_i^j/A_i^k)$, $\mathbf{m}$ is the model vector consisting of $\ln(A_0^j/A_0^k)$ and $\Delta \mathbf{x}_k$, and $\mathbf{G}$ is the kernel consisting of the coefficients of the model vector in the right-hand side of equation (8). We can solve equation (10) by a standard least-squares method if we have more than four observations for each event. Our formulation is essentially the same as that of the master event location method using differences of phase arrival times (Aoki 1974), except we use seismic amplitudes rather than arrival times.

The corresponding model covariance matrix $\mathbf{S}_m$ is

$$\mathbf{S}_m = \left(\mathbf{G}^T \mathbf{S}_d^{-1} \mathbf{G}\right)^{-1}, \tag{11}$$

where $\mathbf{S}_d$ is the data covariance matrix. In the following analysis, we first calculate the variance of data residuals using all events except the reference event. Assuming that errors in the data are independent

each other, we construct a diagonal data covariance matrix with the variance of data residuals to obtain $\mathbf{S}_m$ by equation (11). Because we adopt a common value for variance for all data, the estimation errors of relative source locations derived by equation (11) become the same for all events.

Ichihara and Matsumoto (2017) estimated relative locations of volcanic tremor events using seismic amplitude ratios. They calculated amplitude ratios among several stations to eliminate the source radiation amplitude term ($A_0(f)$ in equation 1) and conducted a grid search to find optimal tremor source locations. It appears that the approach of Ichihara and Matsumoto (2017) estimates relative source locations, because the site amplification terms and intrinsic attenuation factor they used were adjusted to the reference source location. Nevertheless, their principle formulation follows the original ASL method. In contrast, we attribute the amplitude ratio between two events at each station to the relative difference between their locations. Our approach relies on the assumption that the difference between the hypocentral distance of a reference event and a subevent is much smaller than their hypocentral distances, which is not required in the formulation of Ichihara and Matsumoto (2017). Our formulation thus has two advantages over theirs. First, we avoid uncertainties in estimating site amplification factors. Second, our fundamental formulation (equation 8) has a simple linear form, so that we can estimate not only relative source locations, but also the errors on those estimations by using a standard least-squares method.

Data and analysis

Meakandake volcano (eastern Hokkaido, northern Japan; Fig. 1a) has three active craters: Naka-machineshiri, Pon-machineshiri, and Mt. Akanfuji. The eruptive history of Meakandake (Japan Meteorological Agency 2013) shows that its most recent eruption was a phreatic eruption in November 2008 at the 96-1 crater, on the southeastern edge of the Pon-machineshiri crater (Ishimaru et al. 2009). Many earthquakes and tremors were observed before and during the 2008 eruptive period (Ogiso and Yomogida 2012; Japan Meteorological Agency 2013). In this study, we used seismograms of VT earthquakes and volcanic tremors recorded during the 2008 activity at Meakandake by five stations (Fig. 1a) operated by the Sapporo Regional Volcano Observation and Warning Center (RVOWC) of the Japan Meteorological Agency. Vertical-component short-period (natural period 1 s) seismometers were deployed at stations V.PMNS and V.NSYM, and three-component short-period (1 s) seismometers were deployed at the other three stations. Each seismogram was digitized at a sampling rate of 0.01 s.

In this study, we used 1-D velocity and attenuation structure of S-waves shown in Fig. 1b. The velocity structure was derived by trial-and-error approach at Sapporo RVOWC, which has been used there for routine hypocenter determinations since August 2017 (Okuyama, 2020, personal communication). The attenuation structure we used is that of Kumagai et al. (2019), which they used in their application of the ASL method at Nevado del Ruiz volcano (Colombia). We conducted a ray shooting in a spherical coordinate (e.g., Aki and Richards 1980, Chapter 13) to derive $\mathbf{n}_i^j$ in equation (9).

To validate the source locations of the VT earthquakes determined by our new method by comparing them with those determined from phase arrival times, we selected 45 earthquake events that occurred near the 96-1 crater between 1 and 10 November 2008 for which the Sapporo RVOWC had determined hypocenters from phase arrival times. We manually picked up the arrival times of P-waves at all five stations and those of S-waves at stations V.MEAB and V.MNDK (Fig. 2). Note that because the phase arrivals for these earthquakes were clearly evident on all of the seismograms, any event location method using phase arrival times would be suitable for further analysis of this seismic activity. We calculated source locations by three methods: (a) absolute hypocenter estimation from phase arrival times with the HYPOMH algorithm (Hirata and Matsu'ura 1987), (b) master event location estimation (Aoki 1974) using differences of P-wave arrival times, and (c) our new method of estimating relative source locations from seismic amplitudes. The reference event we used for the latter two methods was an earthquake at 21:30 (Japan Standard Time; JST) on 7 November 2008 (latitude 43.3829°, longitude 144.0093°, depth −0.40 km). This reference location was originally determined from the phase arrival times and the HYPOMH algorithm. We selected this reference event because its epicenter was at the centroid of all of the hypocenters derived from the phase arrival times. The P-wave velocity structure we used for the HYPOMH algorithm and master event method was $\sqrt{3}$ times larger than S-wave velocity structure shown in Fig. 1b. For our method of relative source location, we applied a 5–10 Hz bandpass filter to the data of each seismogram, and calculated the root-mean-square (RMS) amplitude of the vertical component within a time window extending for 10 s after the P-wave arrival (Fig. 2). We set frequency f in equation (2) to 7.5 Hz.

For comparison of the calculated volcanic tremor locations, we selected tremors that occurred on 16 and 17 November 2008. Ogiso and Yomogida (2012) applied the ASL method to these events and identified segmentation in their source regions. The duration time of 15 November tremor was about 30 min (Ogiso and Yomogida 2012). Following the approach of Ogiso and Yomogida (2012), we divided the first 18

min of the tremor into three phases (Fig. 3a) and estimated source locations for each phase. During 17 and 18 November, small-amplitude, long-duration tremors were observed intermittently (Ogiso and Yomogida 2012, Fig. 18). Because amplitude ratios among stations did not change significantly during these intermittent tremors (Ogiso and Yomogida 2012, Fig. 21), we estimated tremor locations from 11:00 to 12:00 (JST) on 17 November (Fig. 3b). Because the velocity and attenuation structures we used (Fig. 1b) differed from the simple structures used by Ogiso and Yomogida (2012), we analyzed the locations of these tremors by both the ASL method and our new relative source location method. The process we used to prepare amplitude data was similar to that used for analysis of volcanic earthquakes, apart from the length of the time window. After applying a 5–10 Hz bandpass filter, we calculated the time series of RMS amplitudes from the vertical-component seismogram at each station within a 30-s time window that we shifted by 15 s for each calculation. We then used these time series of RMS amplitudes for both the ASL and our relative source location methods. For the ASL method, we used the same amplification factors as those estimated by Ogiso and Yomogida (2012) using the coda normalization method, and performed a grid search with 0.001˚increments of latitude and longitude and a 0.1 km depth increment. For our relative source location method, we set the reference location at latitude 43.378˚, longitude 144.005˚and 0.1 km depth, which was the tremor location from 01:05:05 to 01:05:35 (JST) on 16 November, as estimated by the ASL method in this study.

Results and discussions

VT earthquakes

Comparison of the hyopcenter distributions of VT earthquakes estimated by the three considered source-location methods (Fig. 4) shows that the focal region derived from phase arrival times extends about 0.5 km horizontally and 1.2 km vertically (Fig. 4a), and that derived by our relative source location method extends about 0.7 km horizontally and 1.0 km vertically (Fig. 4c). The focal region derived by the master event method on the basis of differences of P-wave arrival times (Fig. 4b) had the smallest extent among three results: about 0.2 km horizontally and 0.6 km vertically. We note that the absolute source locations by the master event method and our relative source location method (Figs. 4b and 4c) depended on the location of the selected reference event.

The choice of attenuation structure affected the extent of the focal region for our relative source location method. Equation (8) indicates that an observed amplitude ratio can be decomposed into the ratio of

the source radiation amplitude and the difference in relative source location. Variable B in equation (8) (i.e., the intrinsic attenuation factor in the region of the reference event) determines the contribution of the difference between relative locations to the observed amplitude ratio. If Q is large, the contribution of the difference between relative locations becomes small and the distribution of relative source locations widens. In contrast, the relative source locations converge toward zero with a small value of Q. Ideally, the attenuation structure around the target focal region should be evaluated independently by some other method, such as simultaneous inversion of the source, attenuation and site amplification terms (e.g., Oth et al. 2011; Nakano et al. 2015). Use of a detailed 3-D heterogeneous attenuation structure around a source region (e.g., Matsumoto et al. 2009) would greatly improve the precision of our source location method.

The depth distributions of source locations differ slightly among the three results. The source-depth distribution derived from phase arrival times seems to have a mean of about 0.25 km (Fig. 4a). That derived by the master event method shows most of the sources to be concentrated at about 0 km depth (Fig. 4b). In contrast, the source-depth distribution derived by our relative source location method (Fig. 4c) shows two clusters: the one at about at 0 km and the other at -0.5 km depth. Comparison of this depth distribution to that of the relative source locations derived by the master event method suggests that the shallow source locations derived by our new location method (around -0.5 km depth; Fig. 4c) may not be actual ones. This apparent depth segmentation may be due to two different focal mechanisms. Because the onsets of P- and S-waves for these events were clearly evident in seismograms, their radiation patterns should not be isotropic. If the focal mechanisms of the two events were similar to each other, their spatial distributions of seismic amplitude should also be similar, so the amplitude ratios of the two events well reflect the differences between their source radiation amplitudes and their relative source locations (i.e., equation 5). For events with different focal mechanisms, the amplitude ratios would be dependent on the azimuth of each station. Under such circumstances, equation (5) no longer holds and the results obtained by our new relative source location method may be erroneous. Distortion or reduction of radiation patterns due to multiple scattering of seismic waves (Takemura et al. 2009; Kobayashi et al. 2015) has important ramifications for the ability of our method to stably locate seismic events with different focal mechanisms, as is also the case for the ASL method (Morioka et al. 2017). If the focal mechanisms among events are similar to each other, the relative source locations estimated by seismic amplitude ratios will be equally as reliable as the absolute source locations estimated from phase

arrival times, regardless of the scattering properties of the medium.

Tremors of 16 and 17 November

We now compare the distribution of source locations of volcanic tremors estimated by our method with that estimated by the ASL method. We assumed that the tremors on 16 and 17 November had no clear azimuthal dependency in their spatial distributions of seismic amplitudes. Tremors, which have relatively continuous signals, should be less affected by differences in focal mechanism than the dominant P- and S-wave arrivals of VT earthquakes.

There is a clear southwest to northeast horizontal trend of source locations in all four results (Fig. 5), but their horizontal extents differ. The horizontal extent of source locations obtained using the ASL method are from 1.0 km (Fig. 5c) to 1.5 km (Fig. 5a) whereas those obtained using our new method are from 0.8 km (Fig. 5d) to 1.0 km (Fig. 5b); thus, our method located the tremor sources in more compact regions. Ogiso and Yomogida (2012) found that the tremor locations on 16 November migrated among phases 1, 2, and 3, and that the spatial distribution of phase 3 of the 16 November tremor overlapped those of the following intermittent long-duration tremors on 17 to 18 November. The tremor locations we estimated by the ASL method (Figs. 5a and 5c) show similar characteristics as those of Ogiso and Yomogida (2012, Figs. 15 and 20). They interpreted the location differences of the tremor on 16 November represented downward migration of the tremor source during phases 1 and 2, and that the source region of phase 3 connected the source regions of phases 1 and 2 with those of the following intermittent tremors.

The relative source locations estimated by our new method (Figs. 5b and 5d) show similar overall characteristics to those estimated by the ASL method (Figs. 5a and 5c), but the detail of the spatial relationships of source regions for the three phases of tremor on 16 November differ as follows (Figs. 5a and 5b). Our method showed the source region of the phase 1 tremor to be more tightly concentrated on the western flank of Mt. Akanfuji, with those of phases 2 and 3 a little farther to the northeast of the phase 1 source region, but not extending as far to the northeast as those estimated by the ASL method. In particular, the source region of the phases 2 and 3 overlapped each other. The source region of the tremor of 17 November estimated by our new method was the east of the source regions of the tremor of 16 November, and there was no overlap of the source regions of the events on those two days. This difference between the spatial relationships of the source regions of tremors estimated by the ASL method and our new method may partly reflect to the uncertainty of the site amplification correction in the ASL method. If the site amplification factor at one station differed greatly from its true value,

the source radiation amplitude (equation 3) would also differ from its true value, and the ASL method would then estimate an incorrect source location. If there were many observations (stations), an error in site amplification factor at a single station would be suppressed because equation (3) uses the average of site-corrected amplitudes at all stations. However, the smaller the number of observations (we used only five stations), the larger the influence of each observation on the location estimated by the ASL method. In contrast, our relative source location method minimizes the effect of such errors in site amplification corrections for estimation of source locations. The difference between the source locations derived by the ASL and those derived by our new method demonstrate the ability of our method to cancel out the uncertainties of site amplification factors when there are few stations.

Takahashi et al. (2018) found a region of low resistivity located beneath the northwest flank of Mt. Akan-fuji from audio-frequency magnetotelluric observations, which corresponds to the source regions we identified for three tremor phases on 16 November (Fig. 5b). On the basis of broadband seismic observations, Aoyama and Oshima (2015) retrieved the change of tilt that they attributed to the opening of a vertical crack in the volcanic edifice. To explain the change of tilt, Takahashi et al. (2018) proposed a model in which upward heat convection caused the rapid flow of heat into the low resistivity zone. Migration of the source location, as estimated by the ASL method for the tremor of 16 November, appears to be inconsistent with the model of Takahashi et al. (2018): the descent of the source location between phases 1 and 2 conflicts with the upward heat transfer of their model. In contrast, the relative locations in this study by applying our new method are consistent with their model: the source region of the phase 1 is consistent the activation of volcanic fluids in the low resistivity zone, and the ascent of source locations between phases 2 and 3 is consistent to the rapid transfer of heat from depth.

The locations of the sources of the intermittent tremors (on 17 November) remains controversial. The locations we estimated by the ASL method (Fig. 5c) indicate that the source region of the intermittent tremors partially overlaps that of the phase 3 of the tremor on 16 November (Fig. 5a), whereas our new relative source location method separates the source regions of the two tremors (Figs. 5b and 5d). Based on the source locations estimated by our method, there may have some mechanism by which the two source regions were linked, although no geophysical evidence to support this link has yet come to light. Future improvements in geophysical observation networks around active volcanic craters and greater precision in the location of tremor sources will likely help us to understand the cause of such separations of source regions.

Conclusions

We have presented a new method to estimate relative source locations from seismic amplitudes. The method is similar to the conventional master event method except that it uses event amplitude ratios instead of phase arrival times. Our method avoids the uncertainties inherent in the estimation of site amplification factors by using amplitude ratios between two events at a common station. We assume that for two events near to each other, the observed amplitude ratios can be attributed to the ratio of source radiation amplitude and the difference of relative source location in the form of standard least-squares inversion. As a result, we can use to estimate not only relative source locations but also their errors. The relative source locations of VT earthquakes estimated by our new method showed that using seismic amplitude ratios enabled us to derive a hypocentral distribution similar to that determined by the conventional absolute source location method using phase arrival times. We applied our new method to estimate relative source locations for volcanic tremors recorded at Meakandake volcano on 16 and 17 November 2008, and identified clear segmentation of source clusters and migration of tremor source locations. The observed migration is consistent with other geophysical observations, such as the resistivity structure and changes in tilt determined from broadband seismic data. Our new method of source location from event amplitude data will be useful for detailed analyses of seismic events whose onset times are ambiguous.

Declarations

Ethics approval and consent to participate

Not applicable.

Consent for publication

Not applicable.

List of abbreviations

ASL: Amplitude Source Location

VT: volcano-tectonic

RMS: root-mean-square

RVOWC: Regional Volcano Observation and Warning Center

JST: Japan Standard Time

Availability of data and materials

The waveform data we analyzed are available from the corresponding author on request. The source codes used in this study can be downloaded from https://github.com/mogiso/AmplitudeSourceLocation.

Competing interests

The authors declare that they have no competing interests.

Funding

Not applicable.

Authors' contribution

MO estimated source locations and drafted the manuscript. KY formulated the equations and discussed the results with MO. Both authors read and approved the final manuscript.

Acknowledgments

Sapporo RVOWC provided the waveform data that we used and their current 1-D velocity structure at Meakandake volcano. We used the digital elevation data compiled by the Geospatial Information Authority of Japan. We thank Satoshi Okuyama at Sapporo RVOWC for giving us information about velocity structure and helpful discussions about hypocenter distributions. All figures were drawn with the Generic Mapping Tools version 5 (Wessel et al. 2013).

References

Aki K, Richards PG (1980) Quantitative Seismology Volume 1 and 2, 1st edn. W. H. Freeman and Company, San Francisco

Aoki H (1974) Plate tectonics of arc-junction at central Japan. Journal of Physics of the Earth 22(1):141–161, DOI 10.4294/jpe1952.22.141

Aoyama H, Oshima H (2015) Precursory tilt changes of small phreatic eruptions of Meakan-dake volcano, Hokkaido, Japan, in November 2008. Earth, Planets and Space 67(1), DOI 10.1186/s40623-015-0289-9

Battaglia J (2003) Location of long-period events below Kilauea Volcano using seismic amplitudes and accurate relative relocation. Journal of Geophysical Research 108(B12):2553, DOI 10.1029/2003JB002517

Battaglia J, Aki K (2003) Location of seismic events and eruptive fissures on the Piton de la Fournaise volcano using seismic amplitudes. Journal of Geophysical Research 108(B8):2364, DOI 10.1029/2002JB002193

Battaglia J, Aki K, Ferrazzini V (2005) Location of tremor sources and estimation of lava output using tremor source amplitude on the Piton de la Fournaise volcano: 1. Location of tremor sources. Journal of Volcanology and Geothermal Research 147(3-4):268–290, DOI 10.1016/j.jvolgeores.2005.04.005

Capon J (1969) High-resolution frequency-wavenumber spectrum analysis. Proceedings of the IEEE 57(8):1408–1418, DOI 10.1109/PROC.1969.7278

Doi I, Maeda T (2020) Landslide Characteristics Revealed by High-Frequency Seismic Waves from the 2017 Landslide in Central Japan. Seismological Research Letters 91(5):2719–2729, DOI 10.1785/0220200032

Douglas A (1967) Joint Epicentre Determination. Nature 215(5096):47–48, DOI 10.1038/215047a0

Frémont MJ, Malone SD (1987) High precision relative locations of earthquakes at Mount St. Helens, Washington. Journal of Geophysical Research: Solid Earth 92(B10):10223–10236, DOI 10.1029/JB092iB10p10223

Goldstein P, Archuleta RJ (1987) Array analysis of seismic signals. Geophysical Research Letters 14(1):13–16, DOI 10.1029/GL014i001p00013

Hirata N, Matsu'ura M (1987) Maximum-likelihood estimation of hypocenter with origin time eliminated using nonlinear inversion technique. Physics of the Earth and Planetary Interiors 47(C):50–61, DOI 10.1016/0031-9201(87)90066-5

Ichihara M, Matsumoto S (2017) Relative Source Locations of Continuous Tremor Before and After the Subplinian Events at Shinmoedake, in 2011. Geophysical Research Letters 44(21):10,871–10,877, DOI 10.1002/2017GL075293

Ichimura M, Yokoo A, Kagiyama T, Yoshikawa S, Inoue H (2018) Temporal variation in source location of continuous tremors before ashgas emissions in January 2014 at Aso volcano, Japan. Earth, Planets and Space 70(1):125, DOI 10.1186/s40623-018-0895-4

Ishimaru S, Tamura M, Hirose W, Murayama Y, Okazaki N, Shibata T, Nakagawa M, Yoshimoto M, Hasegawa K, Uesawa S, Nishimoto J, Kosugi A, Matsumoto A, Baba A, Sasaki H, Takahashi

H, Ichiyanagi M, Yamaguchi T, Kohno Y, Honda R, Kasahara M, Sapporo District Meteorological Observatory, Kushiro Local Meteorological Observatory, Abashiri Local Meteorological Observatory (2009) Preliminary report on the eruption on November 2008 of Meakandake volcano. Report of the Geological Survey of Hokkaido 80:115–126 (In Japanese with English figure captions)

Ito A (1985) High resolution relative hypocenters of similar earthquakes by cross-spectral analysis method. Journal of Physics of the Earth 33(4):279–294, DOI 10.4294/jpe1952.33.279

Japan Meteorological Agency (2013) National Catalog of the Active Volcanoes in Japan (the 4th edition, English version). URL https://www.data.jma.go.jp/svd/vois/data/tokyo/STOCK/souran_eng/menu.htm accessed 16 Oct. 2020

Jolly A, Thompson G, Norton G (2002) Locating pyroclastic flows on Soufriere Hills Volcano, Montserrat, West Indies, using amplitude signals from high dynamic range instruments. Journal of Volcanology and Geothermal Research 118(3-4):299–317, DOI 10.1016/S0377-0273(02)00299-8

Klein FW (2002) User's guide to HYPOINVERSE-2000, a Fortran program to solve for earthquake locations and magnitudes. US Geological Survey Open-File Report (02-171):1–123, DOI 10.3133/ofr02171

Kobayashi M, Takemura S, Yoshimoto K (2015) Frequency and distance changes in the apparent P-wave radiation pattern: Effects of seismic wave scattering in the crust inferred from dense seismic observations and numerical simulations. Geophysical Journal International 202(3):1895–1907, DOI 10.1093/gji/ggv263

Kumagai H, Palacios P, Maeda T, Castillo DB, Nakano M (2009) Seismic tracking of lahars using tremor signals. Journal of Volcanology and Geothermal Research 183(1-2):112–121, DOI 10.1016/j.jvolgeores.2009.03.010

Kumagai H, Nakano M, Maeda T, Yepes H, Palacios P, Ruiz M, Arrais S, Vaca M, Molina I, Yamashina T (2010) Broadband seismic monitoring of active volcanoes using deterministic and stochastic approaches. Journal of Geophysical Research: Solid Earth 115(8):1–21, DOI 10.1029/2009JB006889

Kumagai H, Placios P, Ruiz M, Yepes H, Kozono T (2011) Ascending seismic source during an explosive eruption at Tungurahua volcano, Ecuador. Geophysical Research Letters 38(1):2–6, DOI 10.1029/2010GL045944

Kumagai H, Lacson R, Maeda Y, Figueroa MS, Yamashina T, Ruiz M, Palacios P, Ortiz H, Yepes H (2013a) Source amplitudes of volcano-seismic signals determined by the amplitude source location

method as a quantitative measure of event size. Journal of Volcanology and Geothermal Research 257:57–71, DOI 10.1016/j.jvolgeores.2013.03.002

Kumagai H, Pulido N, Fukuyama E, Aoi S (2013b) High-frequency source radiation during the 2011 Tohoku-Oki earthquake, Japan, inferred from KiK-net strong-motion seismograms. Journal of Geophysical Research: Solid Earth 118(1):222–239, DOI 10.1029/2012JB009670

Kumagai H, Londoño JM, Maeda Y, Acevedo Rivas AE (2019) Amplitude Source Location Method With DepthDependent Scattering and Attenuation Structures: Application at Nevado del Ruiz Volcano, Colombia. Journal of Geophysical Research: Solid Earth 124(11):11585–11600, DOI 10.1029/2019JB018156

Kurokawa A, Takeo M, Kurita K (2016) Two types of volcanic tremor changed with eruption style during 1986 Izu-Oshima eruption. Journal of Geophysical Research: Solid Earth 121(4):2727–2736, DOI 10.1002/2015JB012500

Matsumoto S, Uehira K, Watanabe A, Goto K, Iio Y, Hirata N, Okada T, Takahashi H, Shimizu H, Shinohara M, Kanazawa T (2009) High resolution Q^{-1} estimation based on extension of coda normalization method and its application to P-wave attenuation structure in the aftershock area of the 2005 West Off Fukuoka Prefecture Earthquake (M7.0). Geophysical Journal International 179(2):1039–1054, DOI 10.1111/j.1365-246X.2009.04313.x

Morioka H, Kumagai H, Maeda T (2017) Theoretical basis of the amplitude source location method for volcano-seismic signals. Journal of Geophysical Research: Solid Earth 122(8):6538–6551, DOI 10.1002/2017JB013997

Nakano K, Matsushima S, Kawase H (2015) Statistical properties of strong ground motions from the generalized spectral inversion of data observed by K-NET, KiK-net, and the JMA Shindokei network in Japan. Bulletin of the Seismological Society of America 105(5):2662–2680, DOI 10.1785/0120140349

Neidell NS, Taner MT (1971) Semblance and other coherency measures for multichannel data. GEOPHYSICS 36(3):482–497, DOI 10.1190/1.1440186

Obara K (2002) Nonvolcanic deep tremor associated with subduction in southwest Japan. Science 296(5573):1679–1681, DOI 10.1126/science.1070378

Ogiso M, Yomogida K (2012) Migration of tremor locations before the 2008 eruption of Meakandake Volcano, Hokkaido, Japan. Journal of Volcanology and Geothermal Research 217-218:8–20, DOI 10.1016/j.jvolgeores.2011.12.005

445 Ogiso M, Yomogida K (2015) Estimation of locations and migration of debris flows on Izu-Oshima
446 Island, Japan, on 16 October 2013 by the distribution of high frequency seismic amplitudes. Journal
447 of Volcanology and Geothermal Research 298:15–26, DOI 10.1016/j.jvolgeores.2015.03.015
448 Ogiso M, Matsubayashi H, Yamamoto T (2015) Descent of tremor source locations before the 2014
449 phreatic eruption of Ontake volcano, Japan. Earth, Planets and Space 67(1):206, DOI 10.1186/s40623-
450 015-0376-y
451 Oth A, Bindi D, Parolai S, Di Giacomo D (2011) Spectral Analysis of K-NET and KiK-net Data in Japan,
452 Part II: On Attenuation Characteristics, Source Spectra, and Site Response of Borehole and Surface
453 Stations. Bulletin of the Seismological Society of America 101(2):667–687, DOI 10.1785/0120100135
454 Pérez-Guillén C, Tsunematsu K, Nishimura K, Issler D (2019) Seismic location and tracking of snow
455 avalanches and slush flows on Mt. Fuji, Japan. Earth Surface Dynamics 7(4):989–1007, DOI
456 10.5194/esurf-7-989-2019
457 Phillips WS, Aki K (1986) Site Amplification of Coda Waves From Local Earthquakes From Local
458 Earthquakes in Central California. Bulletin of the Seismological Society of America 76(3):627–648
459 Rost S, Thomas C (2002) Array seismology: Methods and applications. Reviews of Geophysics 40(3),
460 DOI 10.1029/2000RG000100
461 Takahashi K, Takakura S, Matsushima N, Fujii I (2018) Relationship between volcanic activity and
462 shallow hydrothermal system at Meakandake volcano, Japan, inferred from geomagnetic and audio-
463 frequency magnetotelluric measurements. Journal of Volcanology and Geothermal Research 349:351–
464 369, DOI 10.1016/j.jvolgeores.2017.11.019
465 Takemoto T, Furumura T, Saito T, Maeda T, Noguchi S (2012) Spatial- and frequency-dependent
466 properties of site amplification factors in Japan derived by the coda normalization method. Bulletin of
467 the Seismological Society of America 102(4):1462–1476, DOI 10.1785/0120110188
468 Takemura S, Furumura T, Saito T (2009) Distortion of the apparent S-wave radiation pattern in the high-
469 frequency wavefield: Tottori-Ken Seibu, Japan, earthquake of 2000. Geophysical Journal International
470 178(2):950–961, DOI 10.1111/j.1365-246X.2009.04210.x
471 Tamaribuchi K, Kobayashi A, Nishimiya T, Hirose F, Annoura S (2019) Characteristics of Shallow
472 LowFrequency Earthquakes off the Kii Peninsula, Japan, in 2004 Revealed by Ocean Bottom Seis-
473 mometers. Geophysical Research Letters 46(23):13737–13745, DOI 10.1029/2019GL085158
474 Waldhauser F, Ellsworth WL (2000) A Double-Difference Earthquake Location Algorithm: Method and

475 Application to the Northern Hayward Fault, California. Bulletin of the Seismological Society of America
476 90(6):1353–1368, DOI 10.1785/0120000006
477 Walsh B, Jolly AD, Procter J (2017) Calibrating the amplitude source location (ASL) method by using
478 active seismic sources: An example from Te Maari volcano, Tongariro National Park, New Zealand.
479 Geophysical Research Letters 44(8):3591–3599, DOI 10.1002/2017GL073000
480 Wessel P, Smith WHF, Scharroo R, Luis J, Wobbe F (2013) Generic Mapping Tools: Improved Version
481 Released. Eos, Transactions American Geophysical Union 94(45):409–410, DOI 10.1002/2013EO450001
482 Yamasato H (1997) Quantitative Analysis of Pyroclastic Flows Using Infrasonic and Seismic Data at
483 Unzen Volcano, Japan. Journal of Physics of the Earth 45(6):397–416, DOI 10.4294/jpe1952.45.397

Figure legends

Figure 1: (a) Regional location map (below) and topographic map (above) of Meakandake volcano showing the locations of the five seismic stations (inverted triangles) used in this study. Topographic contour interval is 50 m. (b) One-dimensional S-wave velocity (left) and attenuation (right) structures used in this study. The origin of the depth is mean sea level.

Figure 2: Waveforms recorded at five stations for a VT earthquake that occurred at 21:30 on 7 November 2008. Vertical and N-S components are shown in black and red, respectively. Gray solid and dashed lines denote P- and S-wave arrival times, respectively. The black double-headed arrows indicate the time windows used to calculate RMS amplitudes.

Figure 3: Vertical component of tremor waveforms recorded at station V.MEAB on (a) 16 November and (b) 17 November 2008. We estimated tremor locations for the waveforms shown in red in (b). Note that both waveforms were decimated without anti-aliasing filtering to reduce the file size of the figure.

Figure 4: Plan and vertical cross-sectional views of the hypocenter distributions of VT earthquakes from 1 to 10 November 2008 derived from (a) phase arrival times and the HYPOMH algorithm, (b) the master event method using differences of P-wave arrival times, and (c) our relative source location method. In panels (b) and (c), estimated location errors are shown in the lower corners. In the plan views, inverted triangles denotes seismic stations, and elevation contours are at 50 m intervals.

Figure 5: Locations of the tremors of (a, b) 16 and (c, d) 17 November as estimated by (a, c) the ASL method and (b, d) our new location method.In (a) and (b), the red, green, and blue stars indicated source locations for the three phases indicated by the same colors in Fig. 3a.

Figures

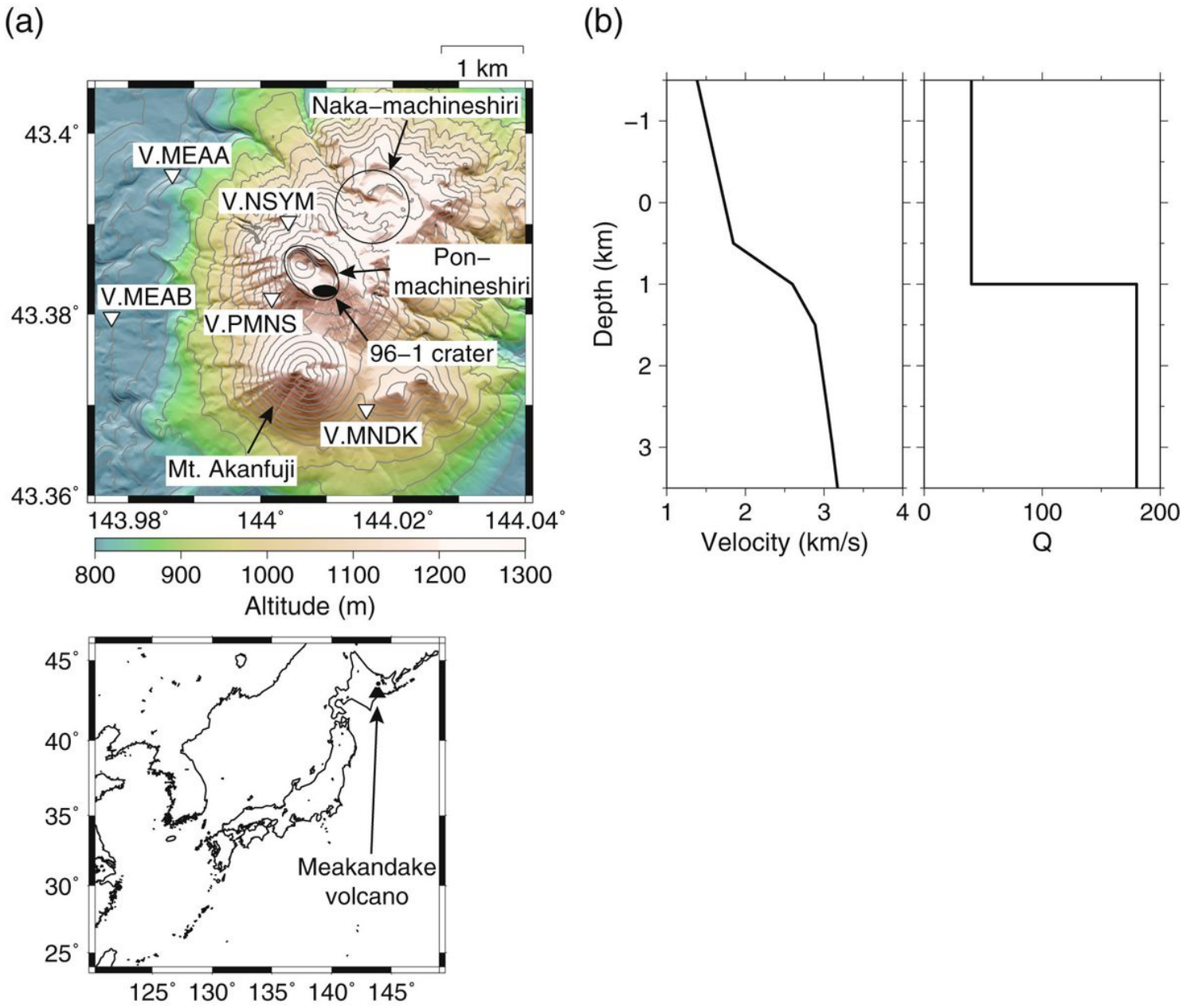

Figure 1

(a) Regional location map (below) and topographic map (above) of Meakandake volcano showing the locations of the five seismic stations (inverted triangles) used in this study. Topographic contour interval is 50 m. (b) One-dimensional S-wave velocity (left) and attenuation (right) structures used in this study. The origin of the depth is mean sea level.

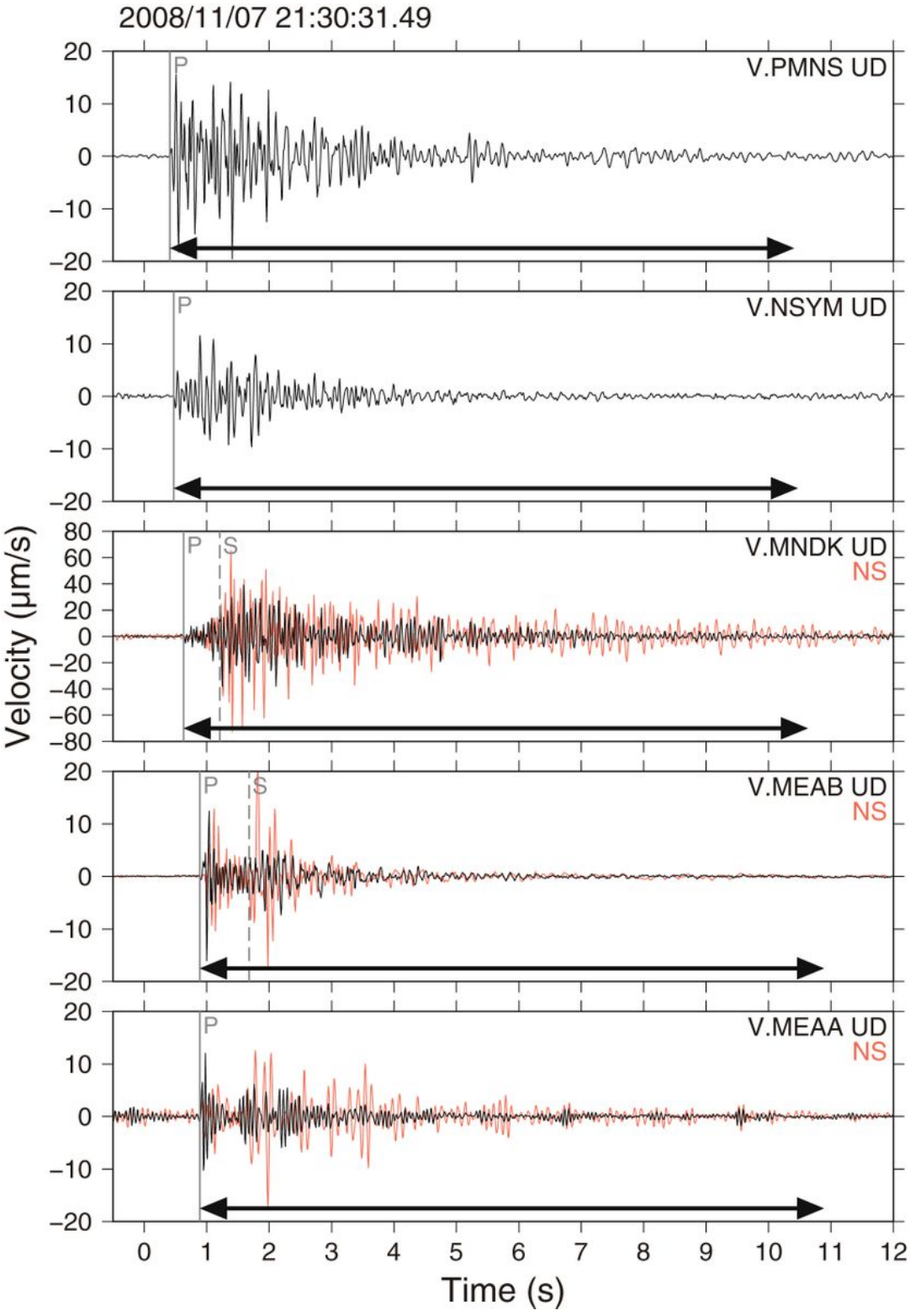

Figure 2

Waveforms recorded at five stations for a VT earthquake that occurred at 21:30 on 7 November 2008. Vertical and N-S components are shown in black and red, respectively. Gray solid and dashed lines denote P- and S-wave arrival times, respectively. The black double-headed arrows indicate the time windows used to calculate RMS amplitudes.

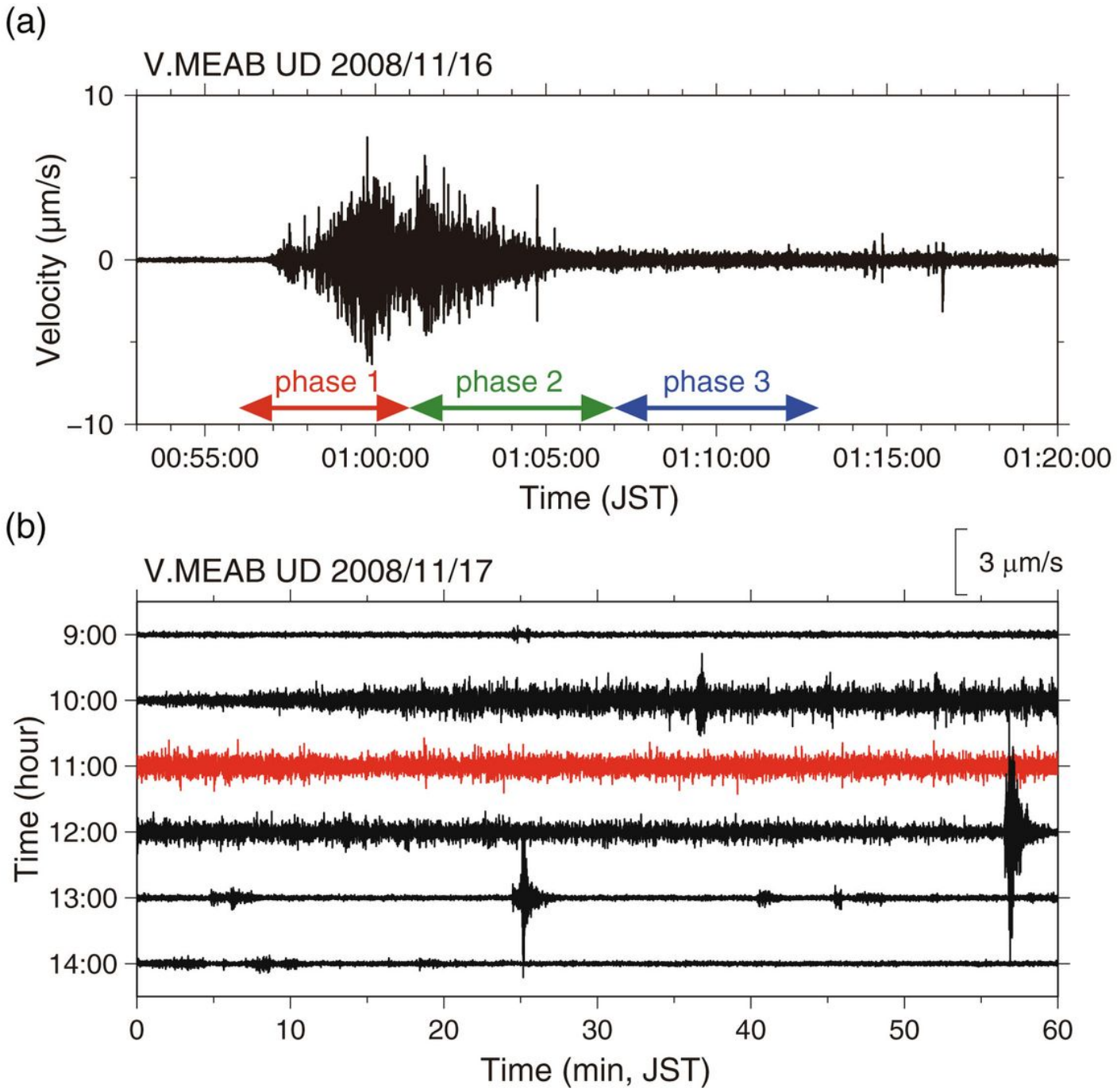

Figure 3

Vertical component of tremor waveforms recorded at station V.MEAB on (a) 16 November and (b) 17 November 2008. We estimated tremor locations for the waveforms shown in red in (b). Note that both waveforms were decimated without anti-aliasing filtering to reduce the file size of the figure.

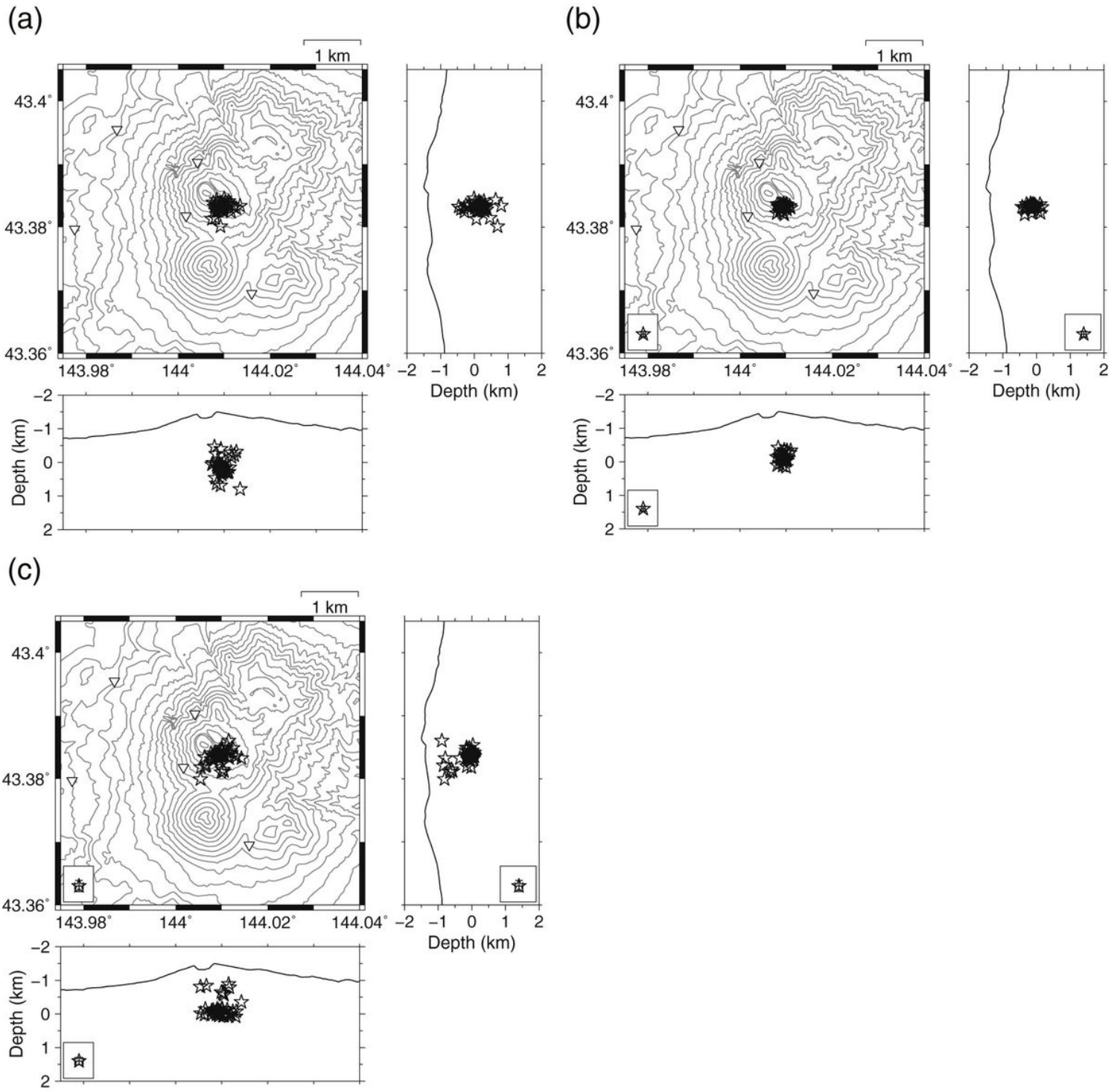

Figure 4

Plan and vertical cross-sectional views of the hypocenter distributions of VT earthquakes from 1 to 10 November 2008 derived from (a) phase arrival times and the HYPOMH algorithm, (b) the master event method using differences of P-wave arrival times, and (c) our relative source location method. In panels (b) and (c), estimated location errors are shown in the lower corners. In the plan views, inverted triangles denotes seismic stations, and elevation contours are at 50 m intervals.

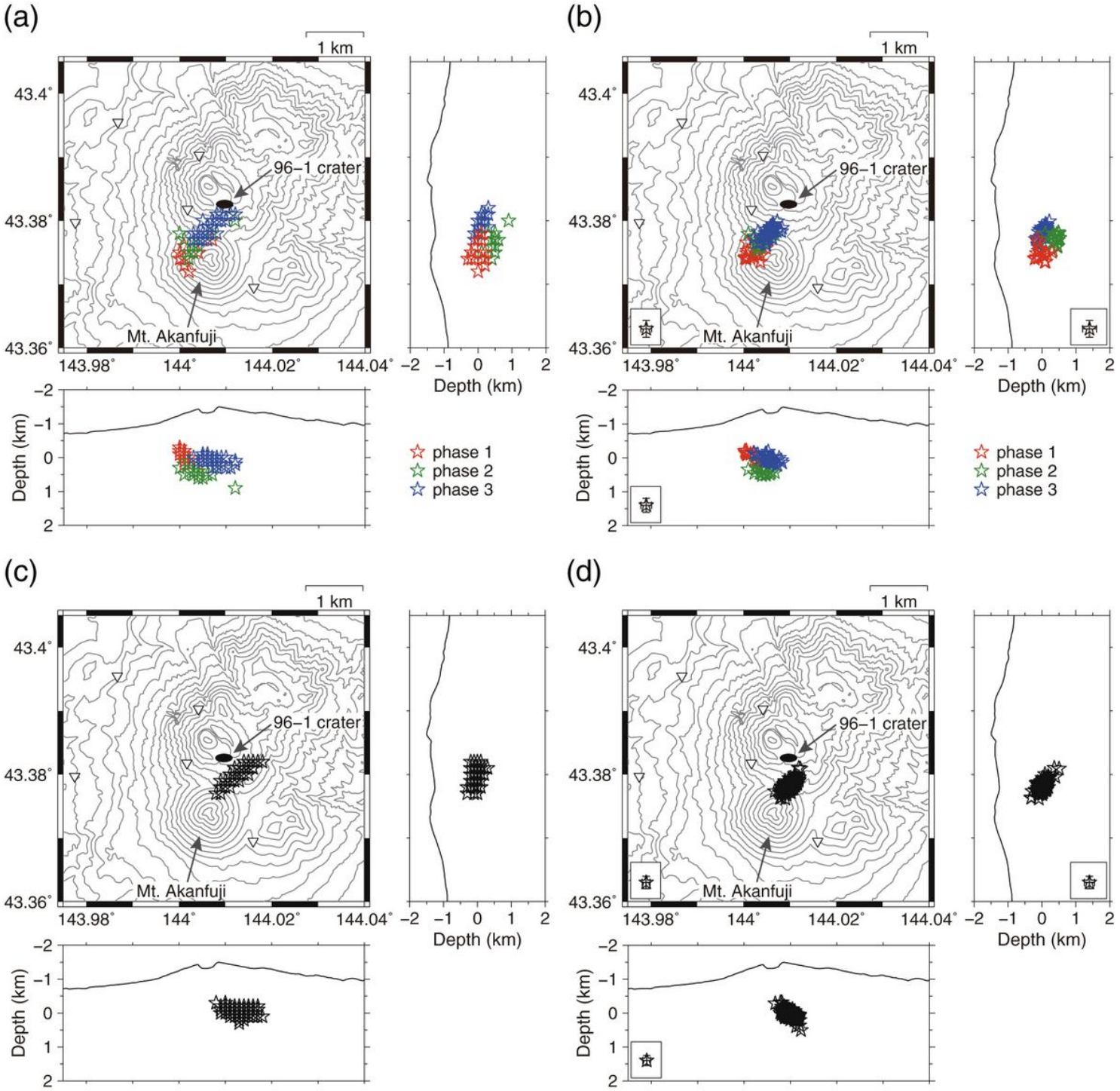

Figure 5

Locations of the tremors of (a, b) 16 and (c, d) 17 November as estimated by (a, c) the ASL method and (b, d) our new location method. In (a) and (b), the red, green, and blue stars indicated source locations for the three phases indicated by the same colors in Fig. 3a.

Supplementary Files

This is a list of supplementary files associated with this preprint. Click to download.

- graphicalabstract.png